Supplementary Material

Source Model and Simulated Strong Ground Motion of the 2021 Yangbi, China Shallow Earthquake Constrained by InSAR Observations

Yongzhe Wang [1,2,*], Kun Chen [1,*], Ying Shi [1], Xu Zhang[1], Shi Chen[1,2], Ping'en Li[1,2], and Donghua Lu [1]

[1] Institute of Geophysics, China Earthquake Administration, Beijing 100081, China; yzwang@cea-igp.ac.cn
[2] Beijing Baijiatuan Earth Science National Observation and Research Station, Beijing 100095, China;
* Correspondence: yzwang@cea-igp.ac.cn; chenkun@cea-igp.ac.cn; Institute of Geophysics, China Earthquake Administration, Beijing 100081, China
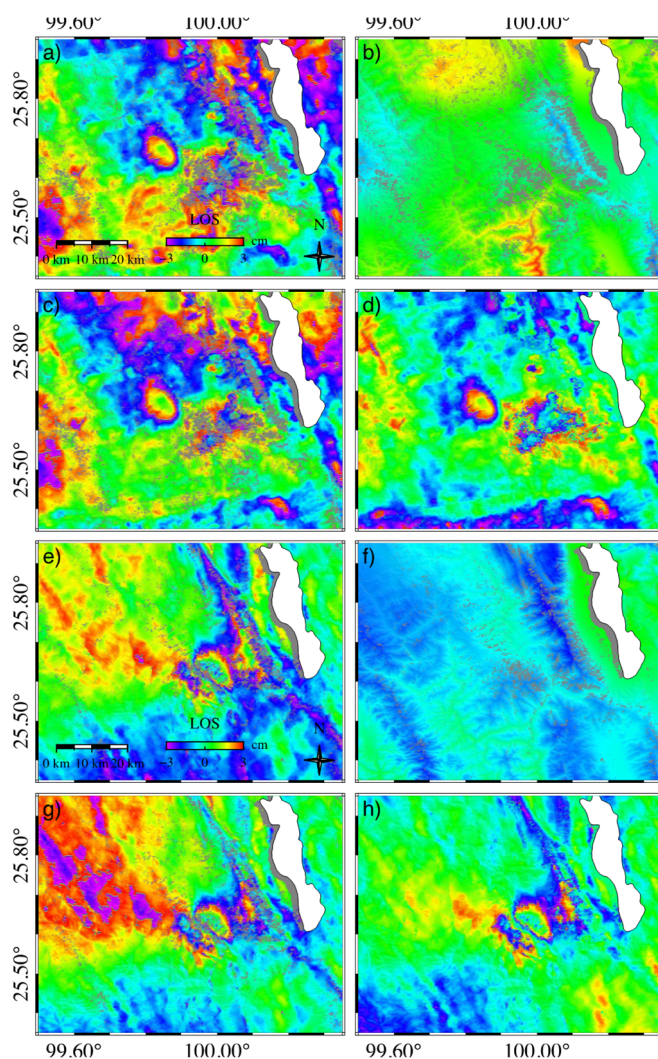
Content of this file

Introduction

This supplement includes additional one table and six figures cited in the main text. Their titles are listed as follows:
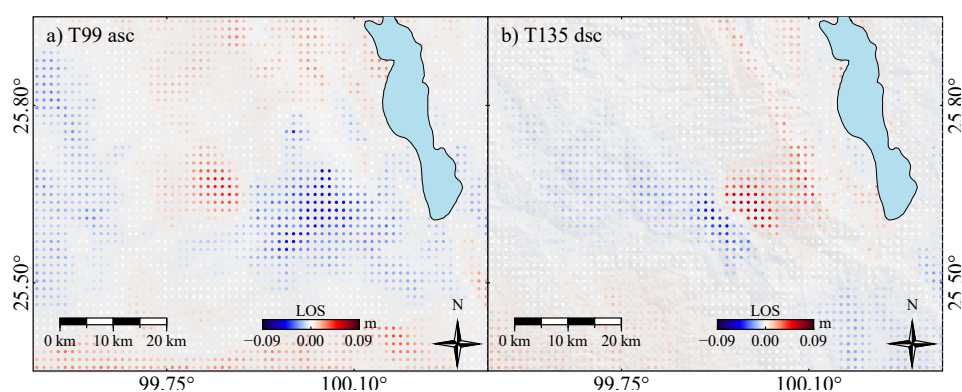
Table S1. Preferred faulting geometric parameters obtained by non-linear inversion.

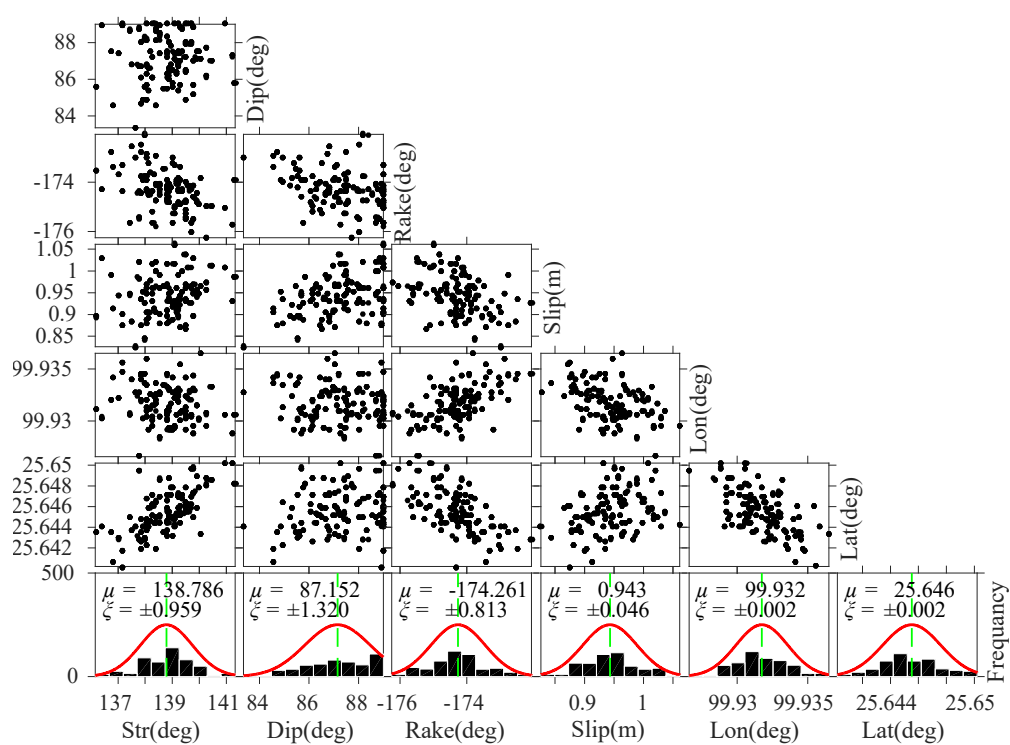| data	Longitude[1] (°)	Latitude[1] (°)	Depth[1] (km)	Length (km)	Width (km)	Strike (°)	Dip (°)	Strike-Slip (m)	Dip-Slip (m)
ASC	99.9449	25.6332	0.03	16	6	134.5	90.0	-0.520	-0.189
DSC	99.9231	25.6532	2.76	12	3	139.2	85.4	-1.244	-0.009
joint	99.9320	25.6460	2.25	14	3	138.8	87.2	-0.935	-0.093

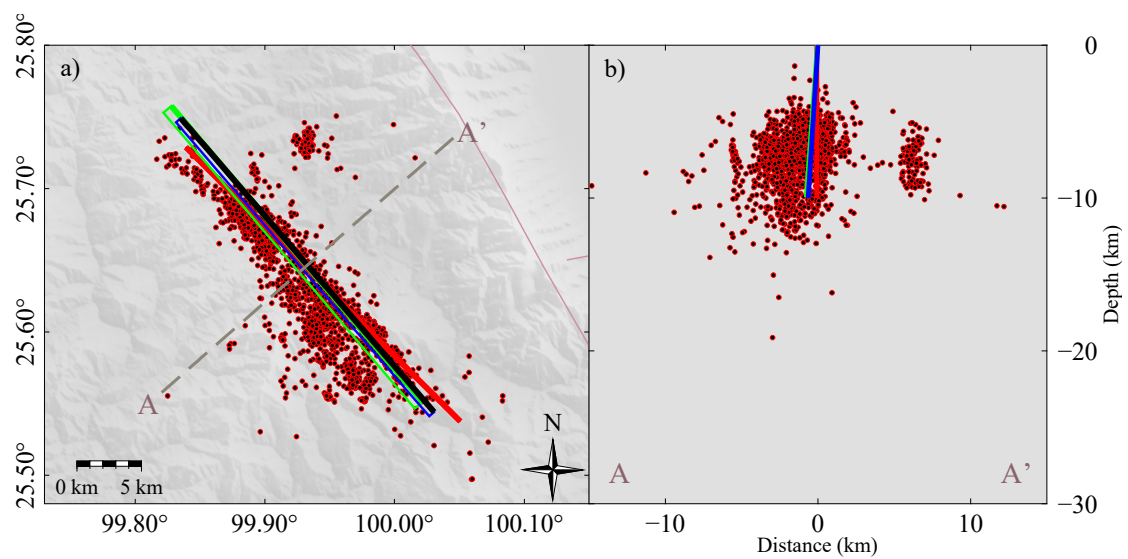[1] Presenting the spatial position of the fault top center.

Figure S1. Refined interferograms of ASC and DSC with atmospheric and orbital errors corrections. One fringe corresponds to a 6 cm surface deformation along the LOS direction. a) and e) are the orig-inal interferograms, b) and f) show the atmospheric interferograms obtained by GACOS, c) and g) are the interferograms after atmos-pheric errors removed, d) and h) are the refined interfero-grams.
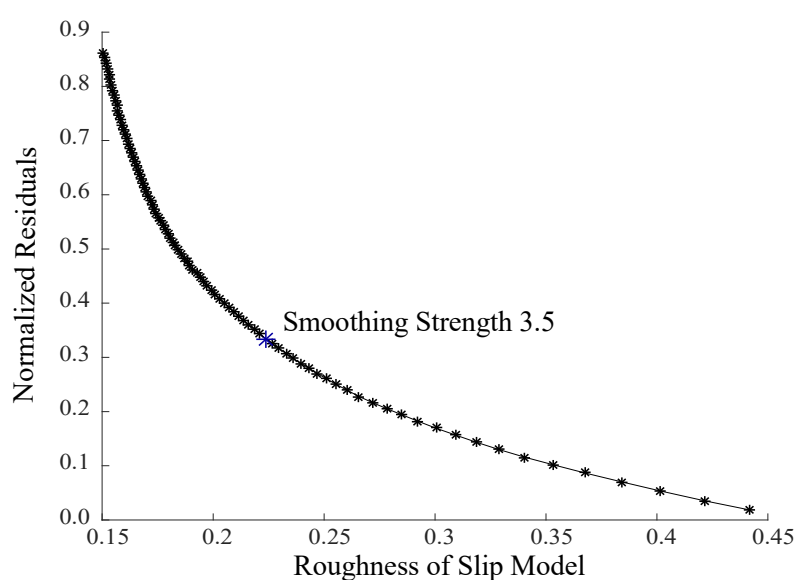
Figure S2. Downsampled InSAR observations. a) for the ASC and b) for the DSC.
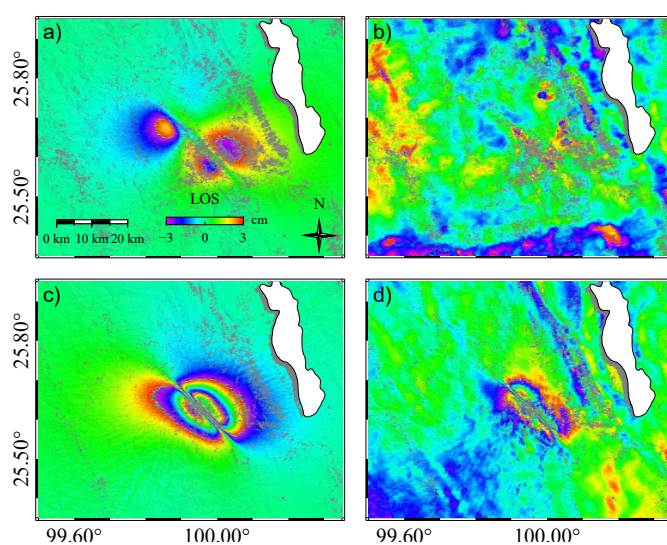
Figure S3. Statistics of the faulting geometric parameters obtained by non-linear inversion.

Figure S4. The spatial relationship between the faulting geometry and the aftershocks. The black line and the blue line are the top line and the plane of the fault inverted by joint inversion. The red line and the green line for the ASC inversion and DSC inversion respectively. a) is the top view of the inverted positions of the fault and the distribution of the aftershocks. Line AA' is the surface horizontal line of profile b). b) is the distribution of aftershocks and the spatial geometry of the fault along the profile AA'.
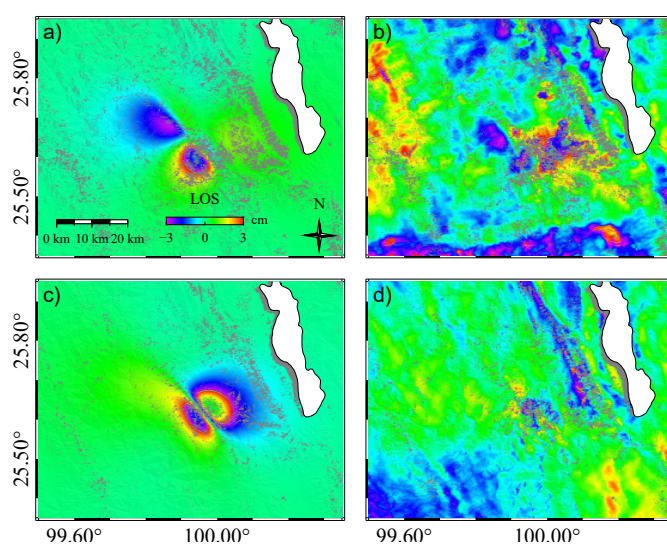
Figure S5. The tradeoff curve between the residual and the roughness. In this study, we selected the smoothing strength 3.5 for all of the model-A, model-D, and model-J.

Figure S6. Simulated and residual interferograms generated by Model-A. a) and b) are the simulated and residual interferograms respectively for the ASC. c) and d) are same to the a) and b) but for the DSC.

Figure S7. Simulated and residual interferograms generated by Model-D. a) and b) are the simulated and residual interferograms respectively for the ASC. c) and d) are same to the a) and b) but for the DSC.